ЯДЕРНА ФІЗИКА ТА ЕНЕРГЕТИКА 2011, т. 12, № 1, с. 7 - 15

УДК 539.172

STRUCTURE PECULIARITIES OF THREE- AND FOUR-CLUSTER NUCLEI ^{6}He, ^{6}Li, AND ^{10}Be, ^{10}C

© 2011 B. E. Grinyuk, I. V. Simenog

M. M. Bogolyubov Institute for Theoretical Physics, National Academy of Sciences of Ukraine, Kyiv

Within a three-particle model ($\alpha + N + N$), structure peculiarities of ^{6}He and ^{6}Li halo nuclei are studied. Within a four-particle model ($\alpha + \alpha + N + N$), the structure of ^{10}Be and ^{10}C nuclei is analized and compared with that of ^{6}He and ^{6}Li. The charge density distributions and form factors of these nuclei are calculated and explained. The density distributions of extra nucleons in ^{10}Be and ^{10}C are studied and compared with the calculated distributions of halo nucleons in ^{6}He and ^{6}Li. A detailed study of the asymptotics of the density distributions is carried out for the three-particle ^{6}He and ^{6}Li nuclei. Asymptotic behavior of the amplitudes of clusterization is analyzed, and the coefficients of clusterization are calculated for the deuteron cluster in ^{6}Li and the dineutron cluster in ^{6}He. The variational method with optimized Gaussian bases is used in calculations.

Keywords: ^{6}He, ^{6}Li, ^{10}Be, ^{10}C, charge density distribution, form factor, coefficient of clusterization.

Introduction

A number of light nuclei are usually treated, from a qualitative point of view, as systems consisting from a few α-particles and some extra nucleons. The physical reason for a successful description of the nuclei within such models is comparatively small binding energies of these systems relative to the α-particle binding energy and comparatively large average distances between clusters. The widely used three-particle model [1, 2] for six-nucleon halo nuclei ^{6}He and ^{6}Li is competitive with the approaches [3, 4] starting from six nucleon degrees of freedom. It is important that, if the parameters of the NN- and $N\alpha$-potentials are fitted to reproduce the energies and radii of the nuclei (in addition to the scattering phase shifts), the three-particle model for ^{6}He and ^{6}Li nuclei becomes [5, 6] a quantitative theory which enables to analyze the structure functions of the nuclei. In this work, we compare some characteristic features of the structure functions of the halo nuclei ^{6}He and ^{6}Li between themselves and with those of ^{10}Be and ^{10}C nuclei, considered within the four-particle model, where two extra nucleons move around two α-particles. In particular, the density distributions and form factors are studied, and the general properties of the probability densities of these nuclei are compared.

We use the variational method with Gaussian bases [7, 8] and the optimization of the bases [5, 6] to achieve a high accuracy in calculations, and we show that this approach allows one to study even the asymptotics of the structure functions [9] in both the coordinate and momentum representations. The obtained asymptotics for the density distributions of particles in ^{6}He and ^{6}Li nuclei are confirmed by analytical estimations. The problem of the asymptotics of form factors is analyzed, and the non-trivial character of the asymptotics for systems with Gaussian potentials is established.

General properties of the structure functions of ^{6}He, ^{6}Li, and ^{10}Be, ^{10}C nuclei

The main properties of the structure functions of ^{6}He and ^{6}Li nuclei are explained within a three-particle model by the presence of two configurations in their wave functions (the "triangle" and "cigar" configurations [1, 2, 5, 6]). In our calculations, we use three-particle Hamiltonians with NN- and $N\alpha$-potentials [5, 6] reproducing the experimental phase shifts at low energies simultaneously with the ground state energies and charge r.m.s. radii of the nucleus under consideration. This is achieved by the use of potentials with local and non-local (separable) terms. A method is developed to calculate phase shifts without a problem of singularities inherent to the variable phase approach with this kind of potentials. To find the structure functions of ^{10}Be and ^{10}C nuclei, we use also an $\alpha\alpha$-potential of the same type (local and non-local terms). This potential, in agreement with the experiment, does not bind the system of two α-particles (^{8}Be), although a small enhancement of the attraction (or switching off the Coulomb repulsion) results in its binding, reproduces (qualitatively) the binding energies of the systems of three (^{12}C) and four (^{16}O) α-particles, and enables one to describe the S-state phase shift of the $\alpha\alpha$-scattering at low energies. In addition, it explains (together with new versions of $N\alpha$-potentials) the binding energy of ^{10}Be (about 8.387 MeV in the four-particle model) and its charge radius 2.357(21) fm. It should be noted that other versions of $\alpha\alpha$-potential (in particular, the Ali-Bodmer potentials [10]) can also be used for studying the structure of ^{10}Be and ^{10}C nuclei. The four-particle approach for studying the ^{10}Be and ^{10}C nuclei may be competitive with the one starting from all the nucleon degrees of freedom [11].

We recall that the variational method with the Gaussian bases [7, 8, 2] enables us to obtain the

wave function $\Phi(\mathbf{r},\boldsymbol{\rho})$ of ^{6}He and ^{6}Li nuclei with high accuracy [5, 6] in an explicit form of a superposition of Gaussian functions suitable for further usage and analysis. In Fig. 1, the probability density $P(r,\rho)=r^2\rho^2\int d\Omega\left|\Phi(\mathbf{r},\boldsymbol{\rho})\right|^2$ is shown for ^{6}He and ^{6}Li nuclei, where r is the distance between the halo nucleons, and ρ is the distance between the α-particle and the center of mass of the halo nucleons. The averaging over the angles is usually done to reduce the number of variables for pictures. In the case of four-particle systems, with one more Jacobi coordinate variable in the four-particle wave function $\Phi(\mathbf{r}_{NN},\boldsymbol{\rho},\mathbf{r}_{\alpha\alpha})$ (where $r_{\alpha\alpha}$ is the relative distance between α-clusters), we make an additional integration over one of them.

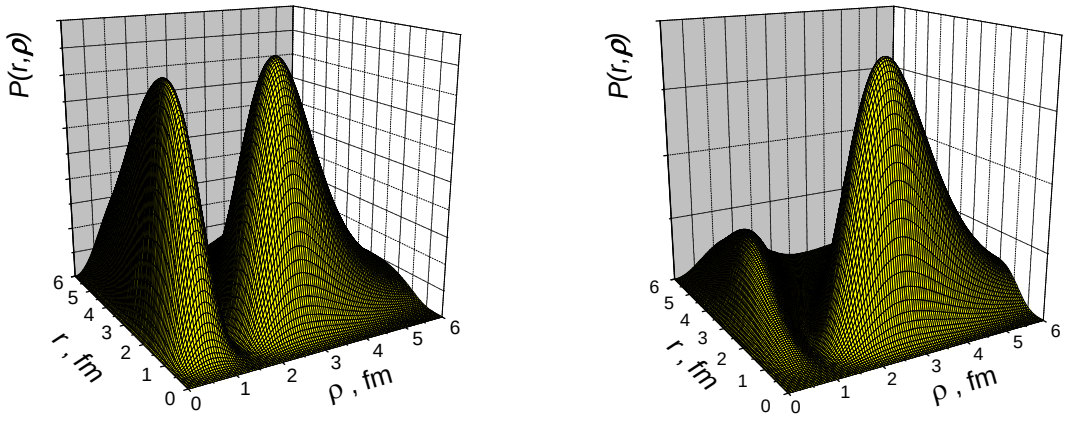

a *b*

Fig. 1. Probability density $P(r,\rho)$ for ^{6}He (*a*) and ^{6}Li (*b*) nuclei in the ground state.

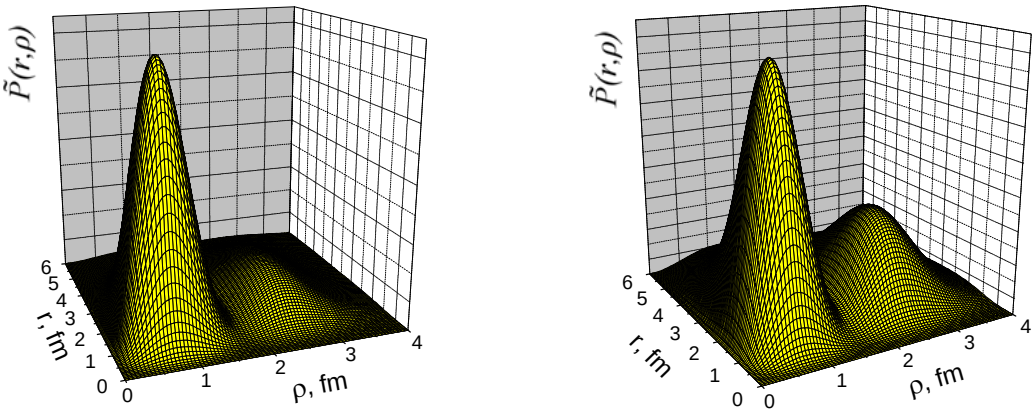

a *b*

Fig. 2. Probability density $\tilde{P}(r,\rho)$ for the extra nucleons of ^{10}Be (*a*) and ^{10}C (*b*) nuclei in the ground state.

In Fig. 2, for ^{10}Be and ^{10}C nuclei, we depict the quantity $\tilde{P}(r,\rho)=r^2\rho^2\int d\Omega\int d\mathbf{r}_{\alpha\alpha}\left|\Phi(\mathbf{r},\boldsymbol{\rho},\mathbf{r}_{\alpha\alpha})\right|^2$ with an additional integration over the relative coordinate $\mathbf{r}_{\alpha\alpha}$ between two α-particles. Here, r is again a distance between extra nucleons, and ρ is the distance between the centers of mass of the two extra nucleons and two α-particles. As it is clearly seen from the figures, the extra nucleons of the both four-particle nuclei also reveal two main configurations: a "cross" one (instead of a "cigar" in the three-particle nuclei), where extra nucleons are at the opposite sides from the α-α axis, and a "tetrahedron" (instead of a "triangle" in ^{6}He and ^{6}Li nuclei), where two extra nucleons form a two-particle cluster moving around the center of mass of the nucleus together with $\alpha\alpha$-cluster. It should be noted that similar probability distribution calculated for α-particles in ^{10}Be or ^{10}C nucleus (with an integration of the wave function squared over $\mathbf{r}_{NN}$) also distinctly shows two peaks.

The specific configurations present in the wave

functions reveal themselves in all the structure functions of these nuclei. The details of the charge and mass density distributions, charge form factors, pair correlation functions, momentum distributions of particles, and amplitudes of clusterization can be found in [5, 6] for ^{6}He and ^{6}Li nuclei (see also reviews [1, 2]). As for four-particle nuclei, we depict only the charge form factor and the charge density distribution of ^{10}Be, and the charge density distribution of ^{10}C. The detailed analysis of the rest structure functions of ^{10}Be, as well as those of ^{10}C, will be published separately. In Fig. 3, *a*, the calculated charge form factor of ^{10}Be is compared with that of ^{6}He nucleus, and with the experimental form factor of ^{4}He. Since neutrons are not charged, the charge form factor of ^{6}He is explained mainly by the presence of an α-particle in this nucleus. In the Helm approximation [12],

$$F_{^6\mathrm{He}}\left(q^2\right) \cong F_{\alpha}\left(q^2\right) \cdot F_{^4\mathrm{He}}\left(q^2\right), \qquad (1)$$

where $F_{\alpha}\left(q^2\right)$ is the form factor of the "point-like" α-particle moving in ^{6}He nucleus, and $F_{^4He}\left(q^2\right)$ is the charge form factor of the α-particle (^{4}He nucleus) itself. In particular, the dip of the charge form factor of ^{6}He is present due to the dip observed in the form factor of ^{4}He (at the same $q^2_{\min}$), while the factor $F_{\alpha}\left(q^2\right)$ is a slowly decreasing function in this region of q^2 [5, 6]. At the same time, a relation similar to Eq. (1), but for the charge form factor of ^{10}Be ($F_{^{10}\mathrm{Be}}\left(q^2\right) \cong F_{\alpha}\left(q^2\right) \cdot F_{^4\mathrm{He}}\left(q^2\right)$, where $F_{\alpha}\left(q^2\right)$ is the form factor of the "point-like" α-particle in ^{10}Be nucleus), results in an additional dip at $q^2_{\min} \sim 5$ fm^{-2}, because $\left|F_{\alpha}\left(q^2\right)\right|$ in the case of ^{10}Be has the dip at this $q^2_{\min}$ due to the structure of the density distribution of two "point-like" α-particles (forming a ^{8}Be cluster) inside ^{10}Be nucleus. The slope of a form factor at the zero transferred momentum is known to be determined by the charge r.m.s. radius of the corresponding nucleus, and the slopes are seen to vary in accordance with the inequality $R_{ch,\,^4He} \cong 1.679$ fm $<$ $R_{ch,\,^6He} \cong 2.068$ fm $<$ $< R_{ch,\,^{10}Be} \cong 2.357$ fm. The difference in radii is obviously observed due to the fact that the charge in ^{6}He is present mainly in the α-particle moving around the center of mass of the nucleus (at an average distance ~ 1.18 fm [5, 6]), while ^{10}Be has two α-particles, each being at an average distance of ~1.65 fm from the center of mass of the nucleus.

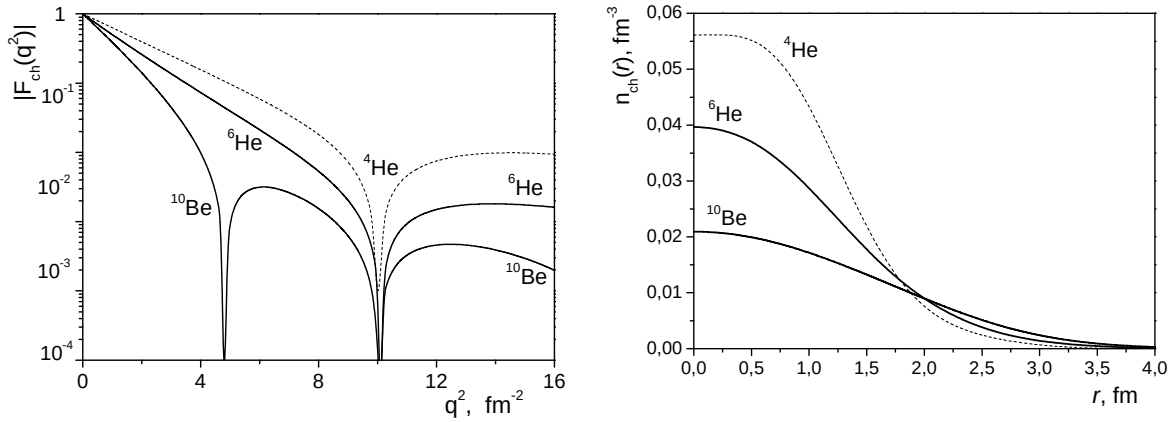

a *b*

Fig. 3. Calculated charge form factors of ^{6}He and ^{10}Be (*a*) and the charge density distributions (normalized to 1) for the same nuclei (*b*). The dashed lines are the interpolations of the experimental data for ^{4}He [13].

In Fig. 3, *b*, the charge density distributions (normalized as $\int n_{ch}\left(r\right) d\mathbf{r} = 1$, where r denotes the distance from the center of mass of a nucleus) are compared for ^{4}He ("free" α-particle), ^{6}He (an α-particle moving around the center of mass of the nucleus), and ^{10}Be (two α-particles forming a ^{8}Be cluster surrounded by two extra neutrons). The calculation of $n_{ch}\left(r\right)$ for ^{6}He is carried out within the Helm approximation

$$n_{ch,\,^6\mathrm{He}}\left(r\right) \cong \int n_{\alpha,\,^6\mathrm{He}}\left(\left|\mathbf{r}-\mathbf{r}_1\right|\right) n_{^4\mathrm{He}}\left(r_1\right) d\mathbf{r}_1, \qquad (2)$$

where $n_{\alpha,\,^6\mathrm{He}}\left(r\right)$ is the calculated density distribution of a "point-like" α-particle in the ^{6}He nucleus [5, 6], and $n_{^4\mathrm{He}}\left(r\right)$ is the experimental charge density distribution [13] of the α-particle itself (with the normalization to 1). In calculations of the ^{10}Be charge density distribution, the expression similar to (2) is used, but with $n_{\alpha,\,^{10}\mathrm{Be}}\left(\left|\mathbf{r}-\mathbf{r}_1\right|\right)$ under

the integral. As it is seen from Fig. 3, *b*, the charge density $n_{ch}(r)$ for ^{10}Be goes lower at short distances than that for ^{6}He nucleus due to the normalization $\int n_{ch}(r)d\mathbf{r} = 1$. If one normalize these distributions to *Z* or *Ze*, then $n_{ch}(r)$ for ^{10}Be should be greater than $n_{ch}(r)$ for ^{6}He at all the distances.

The charge density distribution of ^{10}C is calculated as

$$n_{ch,\,^{10}\mathrm{C}}(r) \cong \frac{2}{3}\int n_{\alpha,\,^{10}\mathrm{C}}\left(\left|\mathbf{r}-\mathbf{r}_1\right|\right) n_{^4\mathrm{He}}(r_1)\, d\mathbf{r}_1 +$$

$$+\frac{1}{3}\int n_{p,\,^{10}\mathrm{C}}\left(\left|\mathbf{r}-\mathbf{r}_1\right|\right) n_p(r_1)\, d\mathbf{r}_1, \qquad (3)$$

where $n_{\alpha,^{10}\mathrm{C}}(r)$ denotes the calculated density distribution of the "point-like" α-particle inside ^{10}C nucleus, $n_{^4\mathrm{He}}(r)$ is the charge distribution of ^{4}He taken from the experiment [13], $n_{p,\,^{10}\mathrm{C}}(r)$ means the calculated density distribution of "point-like" extra protons in ^{10}C, and $n_p(r)$ is the charge distribution of the proton itself derived from the experimental form factor (see, for example, [14]). Note that the charge density distribution of ^{10}C at large distances decreases more slowly than that of ^{10}Be nucleus due to the fact that ^{10}C has a lower binding energy (about 3.73 MeV within the four-particle model), and due to the presence of charged extra protons (Fig. 4). Because of the normalization to unity, $n_{ch}(r)$ of ^{10}C goes lower than $n_{ch}(r)$ of ^{10}Be at intermediate distances, but, near the origin, $n_{ch}(r)$ of ^{10}C is again a little bit greater. If normalized to the charge of the nucleus, $n_{ch}(r)$ of ^{10}C should be, of course, greater than $n_{ch}(r)$ of ^{10}Be at all the distances.

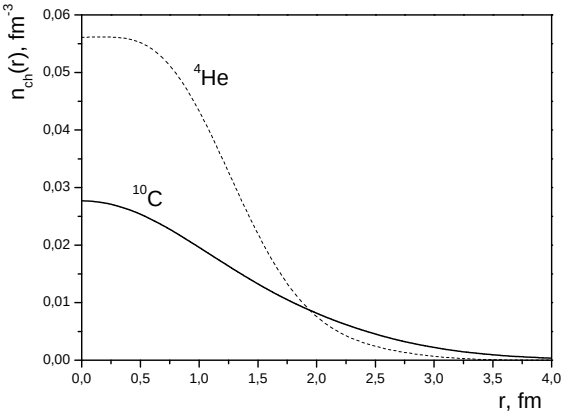

Fig. 4. Calculated charge density distribution (normalized to 1) for ^{10}C nucleus. The dashed line is the interpolation of the experimental data for ^{4}He [13].

Asymptotics of the density distributions in ^{6}He and ^{6}Li nuclei

The asymptotic behavior of the density distributions at large distances from a nucleus determines the sharpness of the nucleus boundary. The asymptotics of the density distributions of particles constituting ^{6}He and ^{6}Li nuclei are essentially different [9] because of different breakup thresholds for these loosely bound near-threshold three-particle systems – the two-particle threshold for ^{6}Li (an α-particle plus a deuteron), and the three-particle threshold for ^{6}He (an α-particle plus two neutrons). It should be noted that, in the case of the asymptotics for ^{6}Li, the decisive role is played by the nearness of the ground state to the two-particle threshold. For example, the asymptotics of the density distributions of the three-nucleon systems [15, 16], due to their greater binding energies, are essentially three-particle ones in spite of the fact that these nuclei have two-particle breakup thresholds.

Consider the density distribution $n_\alpha(r)$ of a "point-like" α-particle in these nuclei (see Fig. 5, *a* for ^{6}Li nucleus; similar dependences for ^{6}He can be found in [9]). In both nuclei, the density $n_\alpha(r)$ has two modes of behavior: the central "core" (≤ 0.5 fm, originated from the "cigar" configuration), and a "halo" (≤ 2.0 fm, arising from the "triangle" configuration). The asymptotic region starts only after $r \ge 2.0$ fm, where the density distribution becomes small. It can be shown [9] that the asymptotics of $n_\alpha(r)$ in ^{6}Li nucleus (having the two-particle threshold) has the form

$$n_{\alpha,\,^6Li}(r) \underset{r\to\infty}{\to} n_{\alpha,\,asymp}(r) \equiv$$

$$\equiv C_\alpha\left(^6Li\right)\frac{W^2_{-\eta,\,\frac{1}{2}}(2\lambda_\alpha\kappa r)}{(2\lambda_\alpha\kappa r)^2} \underset{r\to\infty}{\to} C_\alpha\left(^6Li\right)\frac{\exp(-2\lambda_\alpha\kappa r)}{(2\lambda_\alpha\kappa r)^{2(1+\eta)}}, \qquad (4)$$

where $W_{-\eta,\,\frac{1}{2}}(z)$ is the Whittaker function, $\eta = \dfrac{\mu_{\alpha d}Ze^2}{\hbar^2\kappa} \cong 0.30024$ is the Coulomb parameter, $\kappa = \sqrt{\dfrac{2\mu_{\alpha d}\left|E\left(^6Li\right) - E(d)\right|}{\hbar^2}} \cong 0.3078$ fm^{-1}, and $\lambda_\alpha = \dfrac{m_p + m_n + m_\alpha}{m_p + m_n}$. A comparison of the calculated density distribution $n_\alpha(r)$ with asymptotics (4) gives $C_\alpha\left(^6Li\right) \cong 4.88$ fm^{-2}. In the insert in Fig. 5, *a*, the ratio $n_\alpha(r)/n_{\alpha,\,asymp}(r)$ is shown for ^{6}Li nucleus.

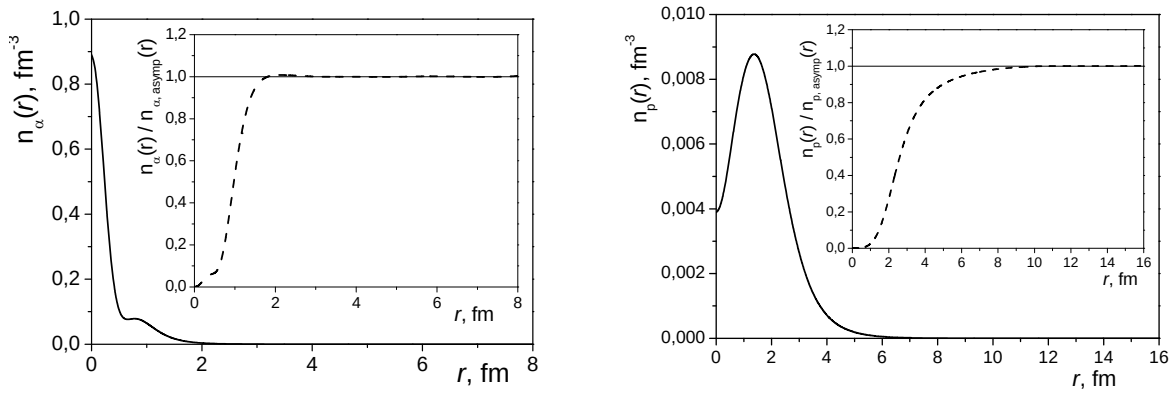

a *b*

Fig. 5. Density distribution $n_\alpha(r)$ of the α-particle in ^{6}Li (*a*), and the halo proton density distribution in the same nucleus (*b*). In the inserts, the corresponding ratios $n(r)/n_{asymp}(r)$ are shown.

It is seen that the asymptotic expression (4) comes into force already after $r \sim 2$ fm. Our variational calculation (with ~300 Gaussian functions) is reliable up to $r \sim 8$ fm, where $n_\alpha(r)$ becomes of the order of ~10^{-9}.

The wave function of ^{6}He nucleus has an essentially different asymptotics [9] (the three-particle Merkuriev's one [17, 18]). As a result, we have for the density distribution $n_\alpha(r)$ of this nucleus

$$n_{\alpha,\,^6\mathrm{He}}(r) \underset{r\to\infty}{\to} n_{\alpha,\,asymp}(r) \equiv \frac{\exp(-ar)}{(ar)^{\frac{5}{2}}}\left(C_{\alpha 0} + \frac{C_{\alpha 1}}{ar} + \ldots\right), \tag{5}$$

where $a = \sqrt{\dfrac{\left|E\left(^6He\right)\right| m_\alpha\left(2m_n + m_\alpha\right)}{\hbar^2 m_n}} \cong 1.491$ fm^{-1}.

A comparison of asymptotics (5) with the result of numerical calculations of $n_{\alpha,\,^6\mathrm{He}}(r)$ enables us to determine the constants $C_{\alpha 0} \cong 0.10$ fm^{-3} and $C_{\alpha 1} \cong 2.43$ fm^{-3}. Since $C_{\alpha 0} << C_{\alpha 1}$, the both terms in relation (5) are competitive at intermediate distances and should be taken into account. The asymptotic dependence (5) is confirmed by our calculations (with ~300 Gaussian functions) up to ~8 fm, where the density decreases to ~10^{-9}.

In the asymptotic expression for the proton density distribution $n_{p,\,^6\mathrm{Li}}(r)$ of ^{6}Li nucleus, one has to keep two competitive terms,

$$n_{p,\,^6\mathrm{Li}}(r) \underset{r\to\infty}{\to} n_{p,asymp}(r) \equiv C_{p1}\left(^6Li\right)\frac{W^2_{-\eta,\,\frac{1}{2}}\left(2\Lambda_{p1}\kappa r\right)}{\left(2\Lambda_{p1}\kappa r\right)^2} +$$

$$+C_{p2}\left(^6Li\right)\frac{\exp\left(-2\Lambda_{p2}\alpha r\right)}{\left(2\Lambda_{p2}\alpha r\right)^2} \underset{r\to\infty}{\to},$$

$$\underset{r\to\infty}{\to} C_{p1}\left(^6Li\right)\frac{\exp\left(-2\Lambda_{p1}\kappa r\right)}{\left(2\Lambda_{p1}\kappa r\right)^{2(1+\eta)}} + C_{p2}\left(^6Li\right)\frac{\exp\left(-2\Lambda_{p2}\alpha r\right)}{\left(2\Lambda_{p2}\alpha r\right)^2}, \tag{6}$$

since the exponential arguments almost coincide due to $\Lambda_{p1}\kappa \cong 0.46286$ fm^{-1} and $\Lambda_{p2}\alpha \cong 0.46294$ fm^{-1} (here, $\alpha = \sqrt{2\mu_{np}\varepsilon_d / \hbar^2}$ is the deuteron parameter, and $\Lambda_{p1} = \dfrac{m_p + m_n + m_\alpha}{m_\alpha}$, $\Lambda_{p2} = \dfrac{m_p + m_n}{m_n}$). The above-mentioned coincidence can be rewritten in terms of energies:

$$E\left(^6Li\right) \cong \frac{\left(m_p + m_n\right)\left(m_n + m_\alpha\right)}{m_n\left(m_p + m_n + m_\alpha\right)}E(d) \approx \frac{5}{3}E(d),$$

which is valid only for ^{6}Li and a deuteron. In Fig. 5, *b*, the density distribution $n_{p,\,^6\mathrm{Li}}(r)$ of the proton in ^{6}Li is shown. In the insert, the ratio between $n_{p,\,^6\mathrm{Li}}(r)$ and its asymptotic (6) is depicted with the use of $C_{p1}\left(^6Li\right) \cong 0.565$ fm^{-3} and $C_{p2}\left(^6Li\right) \cong 0.250$ fm^{-3} determined by a comparison of (6) with the result of numerical calculations of $n_{p,\,^6\mathrm{Li}}(r)$. Similar regularities are valid for the neutron density distribution $n_{n,\,^6\mathrm{Li}}(r)$ in ^{6}Li nucleus [9]. The asymptotics is confirmed by numerical calculations with ~300 basis functions up to ~16 fm, where it becomes ~10^{-9} (or ~10^{-7} as compared with the values near the maximum).

The asymptotic behavior of a halo neutron density distribution $n_{n,\,^6\mathrm{He}}(r)$ in ^{6}He is determined by the three-particle Merkuriev asymptotics [17, 18] of the wave function of the system. It can be shown that the asymptotics of $n_{n,\,^6\mathrm{He}}(r)$ is

$$n_{n,\,^6\mathrm{He}}(r) \underset{r\to\infty}{\to} n_{n,\,asymp}(r) \equiv \frac{\exp(-br)}{(br)^{\frac{5}{2}}}\left(C_{n0} + \frac{C_{n1}}{br} + \ldots\right), \quad (7)$$

where $b = 4\sqrt{\frac{\left|E\left(^6He\right)\right| m_n}{\hbar^2}} \cong 0.61303$ fm^{-1}. The constants $C_{n0} \cong 0.04$ fm^{-3} and $C_{n1} \cong 0.11$ fm^{-3} are determined from a comparison of asymptotics (7) with the result of numerical calculations of $n_{n,\,^6\mathrm{He}}(r)$.

Note that $n_{n,\,^6\mathrm{He}}(r)$ in ^{6}He [5, 6] has no explicit decrease near the origin as the halo proton distribution $n_{p,\,^6\mathrm{Li}}(r)$ in ^{6}Li does, see Fig. 5, *b* (the neutron density distribution $n_{n\,^6\mathrm{Li}}(r)$ in ^{6}Li demonstrates the same decrease). In the both nuclei, the interactions between the halo nucleons were used with an essential repulsion, but it is not the only reason for the decrease under consideration to be present. An additional important reason for this is the fact that the "triangle" configuration is more probable in ^{6}Li than in ^{6}He (see Fig. 1), and this configuration makes small contribution to the density distribution near the origin.

Asymptotics of the amplitudes of clusterization

Consider the amplitude of clusterization [19] for the deuteron in ^{6}Li nucleus

$$f_d(\rho) = \int \phi_d^*(r_{np})\,\Phi(\mathbf{r}_{np}, \boldsymbol{\rho})\, d\mathbf{r}_{np}, \quad (8)$$

which depends on the distance ρ of the α-particle from the center of mass of ^{6}Li. In (8), $\phi_d(r_{np})$ denotes the deuteron wave function, and $\Phi(\mathbf{r}_{np}, \boldsymbol{\rho})$ is the wave function of ^{6}Li nucleus within the three-particle model. The quantity $|f_d(\rho)|^2$ (Fig. 6) is the coefficient of clusterization (see also [20]) reflecting the probability density "to find the deuteron" in ^{6}Li at a definite distance ρ from the α-particle. There are two peaks, distinctly seen in the $\rho^2|f_d(\rho)|^2$ profiles, which correspond to the configurations of "cigar" (short distances) and "triangle" (at ~3 ÷ ÷ 4 fm) present in ^{6}Li (as well as ^{6}He) nuclei. The integral

$$C_d^{(^6Li)} = \int |f_d(\rho)|^2 d\boldsymbol{\rho} \quad (9)$$

gives the probability "to find a deuteron" in the ^{6}Li nucleus. It appears to be 0.69 (about 0.09 is the contribution of the "cigar" (first peak), and about 0.60 comes from the "triangle" (second peak)).

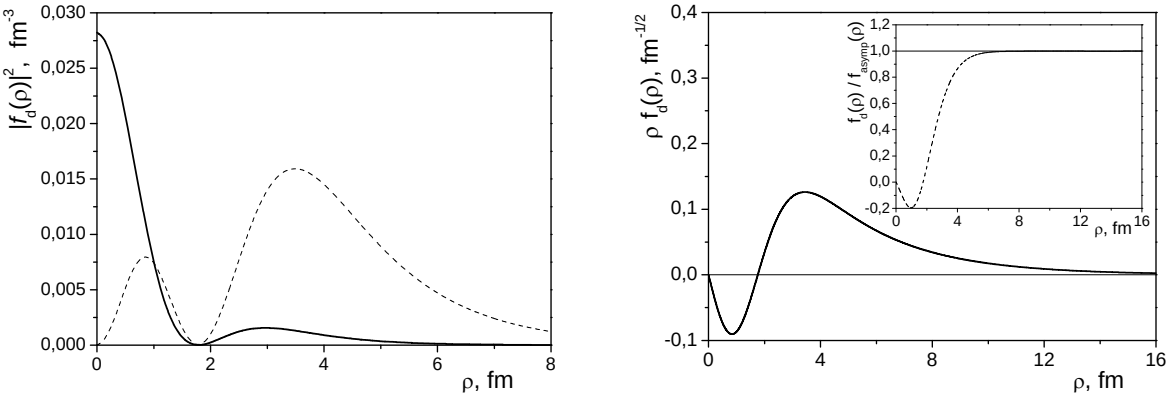

a *b*

Fig. 6. The squared amplitude of clusterization (8) (solid line), and $\rho^2|f_d(\rho)|^2$ (dashed line) for ^{6}Li nucleus (*a*). The same amplitude (8) multiplied by ρ (solid line), and the ratio $f_d(\rho)/f_{asymp}(\rho)$ shown by the dashed line in the insert (*b*).

The deuteron wave function squared is close to the correlation function $g_{np}(r)$ [6], and this is valid not only for the ^{6}Li nucleus but for the most of a few-nucleon systems (see, for example, the calculations for three- and four-nucleon nuclei [15, 21]). Thus, one can consider the modified value $f_{^6Li,\,d-cluster}(\rho)$ similar to (8), where we put $\sqrt{g_{np}(r)}$ instead of $\phi_d(r)$. Then the value $|f_{^6Li,\,d-cluster}(\rho)|^2$ is to be the "deuteron cluster" coefficient of clusterization. Its profile is close to $|f_d(\rho)|^2$ (see [6]). The corresponding modified

coefficient $C^{(^6Li)}_{d-cluster}$ is defined by the relation similar to (9), and it is equal to 0.74 (0.08 due to the "cigar" configuration, and 0.66 comes from the "triangle"). The modified coefficients of clusterization enable one to estimate the probability for the dineutron cluster to exist in a ^{6}He nucleus, although a free dineutron does not exist. We find the coefficient $C^{(^6He)}_{nn-cluster}$ = 0.73. It is natural that the "cigar" configuration plays somewhat greater role in ^{6}He than that in ^{6}Li, because the *np* subsystem in ^{6}Li prefer to be a deuteron cluster, because V_{np} in the triplet state is (on average) more attractive than V_{nn} in the singlet state.

The analysis of the asymptotics of amplitude (8) is of a special interest due to the fact [2, 20] that it determines the asymptotic constant for the process $^6\text{Li} \to \alpha + d$ and, as a result, the corresponding nuclear vertex constant and the spectroscopic factor. The asymptotical behavior of (8) is known to be

$$f_d(\rho) \underset{\rho\to\infty}{\to} f_{d,asymp}(\rho) \equiv C_A \rho^{-1} W_{-\eta,\frac{1}{2}}(2\kappa\rho) \underset{\rho\to\infty}{\to}$$

$$\underset{\rho\to\infty}{\to} C_A \rho^{-1} \exp\left(-\kappa\rho - \eta \ln(2\kappa\rho)\right) \qquad (10)$$

(the notation is the same as in (3)). In Fig. 6, *b*, we show the ratio $f_d(\rho)/f_{asymp}(\rho)$ calculated for one of the sets of potentials proposed in [6] (the dashed line). Comparing the results of our calculation of $f_d(\rho)$ (reliable up to $\rho \sim 15$ fm with 300 Gaussian functions of the basis used) with the asymptotics (10) (coming into force already at ~6 fm), we have $C_A = 0.693$ fm$^{-1/2}$, or $\sqrt{4\pi}\ C_A = 2.46$ fm$^{-1/2}$, and this is consistent with other calculations [2].

Some remarks about the asymptotics of form factors

Recently, we have analyzed and explained the form factors of ^{6}Li and ^{6}He nuclei in details both at low and high transferred momenta [9]. A special attention is paid to the problem of the asymptotics of the form factors of ^{6}Li and ^{6}He nuclei. It is shown that, even within a non-relativistic problem and commonly used interaction potentials, the asymptotics of the form factors is a non-trivial problem. For rapidly decreasing (in the momentum representation) potentials, the asymptotics of a form factor cannot be expressed as $\sim\left(\frac{v(q)}{q^2}\right)^{A-1}$ [22], which is valid only for slowly decreasing $v(q)$. For rapidly decreasing potentials, the problem is much more sophisticated even for a two-particle system, nothing to say about the many-body ones. For example, for the attractive Gaussian potential $V(r) = -g\exp\left(-(r/r_0)^2\right)$, it can be shown for the two-particle wave function in the momentum representation to have the asymptotic behavior

$$\psi(p) \underset{p\to\infty}{\to} \frac{C}{p\sqrt{p^2+\alpha^2}} \exp\left(-r_0 \int\limits_{Const}^{\frac{1}{2}r_0 p} \sqrt{\ln\left(\frac{q^2+\alpha^2}{g}\right)}\, dq\right) \qquad (11)$$

(here, $\alpha^2 \equiv 2\mu|E|/\hbar^2$). The proof of this fact, and the results for the general case of an arbitrary potential will be considered separately. And this asymptotical dependence of the wave function determines the asymptotics of the formfactor $F(q) = \int \psi^*(p)\psi\left(\left|\mathbf{p} + \frac{m_2}{m_1+m_2}\mathbf{q}\right|\right)\frac{d\mathbf{p}}{(2\pi)^3}$ which differs essentially from $\sim\left(\frac{v(q)}{q^2}\right)^{A-1}$ [22].

To summarize, we note that the developed approach enables us to study the structure functions of light nuclei and to analyze the asymptotics of these structure functions both in the coordinate and momentum representations. Considering α-clusters like α-particles, and appropriately fitting α-α- and α-nucleon potentials, one can essentially simplify the many-body problem without significant lost of accuracy in studying the structure of a number of light nuclei.

This work is partially supported by a target program of the Division of Physics and Astronomy of the National Academy of Sciences of Ukraine.

REFERENCES

1. *Zhukov M. V., Danilin B. V., Fedorov D. V. et al.* Bound State Properties of Borromean Halo Nuclei: ^{6}He and ^{11}Li // Physics Reports. - 1993. - Vol. 231, No. 4. - P. 151 - 199.
2. *Kukulin V. I., Pomerantsev V. N., Razikov Kh. D. et al.* Detailed Study of the Cluster Structure of Light Nuclei in a Three-Body Model (IV). Large Space Calculation for *A* = 6 Nuclei with Realistic Nuclear Forces // Nucl. Phys. - 1995. - Vol. A 586, No. 1. - P. 151 - 189.
3. *Василевский В. С., Нестеров А. В., Арикс Ф., Ван Лёувен П.* Трехкластерный вариант алгебраиче-

ской версии метода резонирующих групп и его применение к исследованию свойств связанных состояний ядер ^{6}He и ^{8}He // Зб. наук. праць Ін-ту ядерних досл. - 2002. - № 2(8). - С. 51 - 59.

4. *Вербицкий В. П., Поздняков Ю. А., Теренецкий К. О.* Вариационный расчет энергии основного состояния ядра ^{6}He в трехкластерном приближении метода резонирующих групп // Изв. РАН. Сер. физ. - 1996. - Т. 60, № 1. - С. 52 - 57.
5. *Гринюк Б. Е., Сименог И. В.* Структура ядра ^{6}He в трехчастичной модели // Ядерная физика. - 2009. - Т. 72, № 1. - С. 10 - 24; *Grinyuk B. E., Simenog I. V.* Structure of the ^{6}He Nucleus in the Three-Particle Model // Phys. Atomic Nuclei. - 2009. - Vol. 72, No. 1. - P. 6 - 19.
6. *Grinyuk B. E., Simenog I. V.* Three-Particle Structure of the Halo Nucleus ^{6}Li // Nuclear Physics and Atomic Energy. - 2009. - Vol. 10, No. 1. - P. 9 - 19.
7. *Kukulin V. I., Krasnopol'sky V. M.* A Stochastic Variational Method for Few-Body Systems // J. Phys. G: Nucl. Phys. - 1977. - Vol. 3, No. 6. - P. 795 - 811.
8. *Suzuki Y., Varga K.* Stochastic Variational Approach to Quantum-Mechanical Few-Body Problems. - Springer, Berlin, 1998.
9. *Grinyuk B. E., Simenog I. V.* Asymptotic Features of Density Distributions and Form Factors for ^{6}Li and ^{6}He Nuclei within the Three-Particle Model // Ukr. J. Phys. - 2010. - Vol. 55, No. 4. - P. 369 - 380.
10. *Ali S., Bodmer A. R.* Phenomenological α-α Potentials // Nucl. Phys. - 1966. - Vol. 80. - P. 99 - 112.
11. *Ogawa Y., Arai K., Suzuki Y., Varga. K.* Microscopic Four-Cluster Description of ^{10}Be and ^{10}C with the Stochastic Variational Method // Nucl. Phys. - 2000. - Vol. A 673, No. 1. - P. 122 - 142.
12. *Akhiezer A. I., Sitenko A. G., Tartakovsky V. K.* Nuclear Electrodynamics. - Springer, Berlin, 1994.
13. *Frosch R. F., McCarthy J. S., Rand R. E., Yearian M. R.* Structure of the ^{4}He Nucleus from Elastic Electron Scattering // Phys. Rev. - 1967. - Vol. 160, No 4. - P. 874 - 879.
14. *P. E. Bosted et al*. Measurements of the Electric and Magnetic Form Factors of the Proton from $Q^2 = 1.75$ to 8.83 $(\mathrm{GeV/c})^2$ // Phys. Rev. Lett. - 1992. - Vol. 68, No 26. - P. 3841 - 3844.
15. *П'ятницький Д. В., Сименог І. В.* Кореляційні функції, імпульсні розподіли та коефіцієнти кластеризації для тринуклонних ядер // Ядерна фізика та енергетика. - 2009. - Т. 10, № 1. - С. 36 - 44.
16. *П'ятницький Д. В., Сименог І. В.* Асимптотики розподілів густини, імпульсних розподілів та формфакторів тринуклонних ядер // Ядерна фізика та енергетика. - 2010. - Т. 11, № 1. - С. 16 - 24.
17. *Меркурьев С. П.* Об асимптотическом виде трехчастичных волновых функций дискретного спектра // Ядерная физика. - 1974. - Т. 19, № 3. - С. 447 - 461.
18. *Faddeev L. D., Merkuriev S. P.* Quantum Scattering Theory for Several Particle Systems. - Kluwer, Dordrecht, 1993.
19. *Filippov G. F., Ovcharenko V. I., Simenog I. V.* Cluster Structure of the Three-Particle Bound State. - Kiev, 1971. - 46 p. - (Preprint / ITP-71-74E).
20. *Блохинцев Л. Д., Борбей И., Долинский Э. И.* Ядерные вершинные константы // ЭЧАЯ. - 1977. - Т. 8, вып. 6. - С. 1189 - 1245.
21. *Grinyuk B. E., Piatnytskyi D. V., Simenog I. V.* Structure Characteristics of a ^{4}He Nucleus within the Microscopic Approach // Ukr. J. Phys. - 2007. - Vol. 52, No. 5. - P. 424 - 435.
22. *Amado R. D., Woloshyn R. M.* Momentum Distributions in the Nucleus // Phys. Lett. - 1976. - Vol. 62 B, No 3. - P. 253 - 255.

СТРУКТУРНІ ОСОБЛИВОСТІ ТРИ- І ЧОТИРИКЛАСТЕРНИХ ЯДЕР ^{6}He, ^{6}Li ТА ^{10}Be, ^{10}C

Б. Є. Гринюк, І. В. Сименог

Досліджено особливості структури ядер ^{6}He і ^{6}Li в рамках тричастинкової моделі ($\alpha + N + N$). На основі чотиричастинкової моделі ($\alpha + \alpha + N + N$) проаналізовано структуру ядер ^{10}Be і ^{10}C і порівняно зі структурою ^{6}He і ^{6}Li. Розраховано й пояснено розподіли зарядової густини і форм-фактори зазначених ядер. Досліджено розподіли густини екстрануклонів у ^{10}Be і ^{10}C та порівняно з розрахованими розподілами нуклонів гало ядер ^{6}He і ^{6}Li. Виконано детальне дослідження асимптотик розподілів густини в ядрах ^{6}He і ^{6}Li. Проаналізовано асимптотичну поведінку амплітуд кластеризації та обчислено коефіцієнти кластеризації для дейтронного кластера в ^{6}Li і дінейтронного кластера в ^{6}He. У розрахунках використано варіаційний метод з оптимізованими гауссоїдними базисами.

Ключові слова: ^{6}He, ^{6}Li, ^{10}Be, ^{10}C, розподіл густини заряду, форм-фактор, коефіцієнт кластеризації.

СТРУКТУРНЫЕ ОСОБЕННОСТИ ТРЕХ- И ЧЕТЫРЕХКЛАСТЕРНЫХ ЯДЕР ^{6}He, ^{6}Li И ^{10}Be, ^{10}C

Б. Е. Гринюк, И. В. Сименог

Изучены особенности структуры ядер ^{6}He і ^{6}Li в рамках трехчастичной модели ($\alpha + N + N$). На основе четырехчастичной модели ($\alpha + \alpha + N + N$) проанализирована структура ядер ^{10}Be и ^{10}C и проведено сравнение со структурой ^{6}He и ^{6}Li. Рассчитаны и объяснены распределения зарядовой плотности и форм-факторы упомянутых ядер. Исследованы распределения плотности экстрануклонов в ^{10}Be и ^{10}C и сравнены с рассчитанными распределениями нуклонов гало в ядрах ^{6}He и ^{6}Li. Проанализировано асимптотическое поведение амплитуд кластеризации и вычислены коэффициенты кластеризации для дейтронного кластера в ^{6}Li и динейтронного кластера в ^{6}He. В расчетах использован вариационный метод с оптимизированными гауссоидальными базисами.

Ключевые слова: ^{6}He, ^{6}Li, ^{10}Be, ^{10}C, распределение плотности заряда, форм-фактор, коэффициент кластеризации.

Received 08.12.10,
revised - 11.03.11.